

# Modeling of Three-dimensional Unsteady Wake Past a Large Migratory Bird during Flapping Flight

BEAUMONT F., BOGARD F., MURER S., POLIDORI G. MATIM

University of Reims Champagne Ardenne

Faculty of Exact and Natural Science

FRANCE

**Abstract:** This preliminary study aimed to model the aerodynamic behavior of a large migratory bird during a forward flapping flight. Computational Fluid Dynamics (CFD) was used to model the flow around and in the wake of a Canada Goose flying at an altitude of 1000m and a speed of 13.9m/sec. Flapping of the wings was modeled through dynamic meshing and subroutines implemented in a computational code using the Finite Volumes method. Monitoring of the flow quantities during the unsteady calculation revealed a close relationship between the wing-flapping dynamics and the cyclic variation of the forces acting on the bird. Post-processing of the 3D results revealed a complex flow pattern mainly composed of two contra-rotating vortices developing at the wingtip. In a perpendicular plane to the main flow direction, we demonstrated that the bird's wake can be divided into two distinct zones: the downwash zone and the upwash zone. The latter is used by birds flying in formation to reduce their energy expenditure. We have also shown that when the bird flaps its wings, the trail of upwash left by the wingtips moves up and down in a wave-like motion. Further studies, which will include several birds, will be necessary to understand all the aerodynamic implications related to the flight of migratory birds in formation.

**Key-Words:** Computational Fluid Dynamics (CFD), Vortex, wake, flapping wings, migratory birds, upwash, downwash

Received: April 12, 2021. Revised: January 8, 2022. Accepted: January 20, 2022. Published: March 1, 2022.

## 1 Introduction

Many animal species travel in highly organized groups [1-3]. According to many studies, the primary interest of such formations would be to reduce energy expenditure and improve the locomotor performance of the animals in the group [4-11]. Among the organized groups, the V-shaped formation IS so characteristic of bird flights THAT has always intrigued researchers and continues to interest not only scientists but also many people who enjoy this lively spectacle [4, 7, 9-12]. Research on the topic shows that when birds are flying in a group, there is an energetic advantage to birds flying behind and next to another bird by using the areas of eddies generated by the wings of the bird preceding it [4, 7, 9-11]. However, a definitive understanding of the aerodynamic implications of these formation flights is still difficult to establish. Aerodynamic models are nevertheless of great interest to ecologists who are trying to understand the strategies and constraints related to the migration of wild birds. For many years, scientists have been striving to study the mechanics of bird flight, whether from a biomechanical or aerodynamic point of view. As precursors, Magnan et al. [13] used tobacco smoke

to visualize the whirling wake of a Columba livia pigeon and discovered that when a bird flew slowly, the wake consisted of vortex loops. Although the published photographs are quite blurred and difficult to interpret, it was the first demonstration that the sheet of vortices curled into discrete structures associated with the wing flapping cycle. More recently, some authors [15-16] have applied a digital particle image velocimetry (DPIV) technique to bird flight. However, this experimental technique requires both the use of a low-turbulence wind tunnel and a cooperative and well-trained bird. For these reasons, no quantitative studies on the wakes of large high-speed flying birds have been published to date [17]. An alternative to experimental techniques is computational fluid dynamics (CFD). Numerical simulations are often less expensive and less constraining than laboratory experiments while providing all flow quantities, including those that are generally not accessible from measurements. CFD has been used by scientists to model wing flapping and improve understanding of the mechanics of bird flight. Maeng et al. [12] conducted a numerical study of the energy savings of Canada geese in flight. More recently, Song et al.

[18] studied the aerodynamics of the flapping wings of a calliope hummingbird using a dynamic meshing method to reproduce the wing-flapping motion. These studies show that CFD is an interesting and complementary alternative to classical flow visualization methods and can be applied to the study of complex vortex wakes.

This preliminary study is an essential step in understanding the aerodynamic mechanisms related to the cooperative flight of migratory birds. In this work, we have developed a computational method based on three-dimensional numerical simulations that integrate realistic wing flapping kinematics. For these purposes, Computational Fluid Dynamics (CFD) code was used to model the flow around and in the wake of a Canada goose flying at an altitude of 1000 m and a speed of 13.9 m/sec. Wing flapping dynamics were modeled through a dynamic mesh and sub-program implementation. To our best knowledge, this study is the first to provide a detailed and realistic representation of the unsteady three-dimensional wake of a large migratory bird during a flapping flight.

## 2 Methods

### 2.1 Geometry and Computational Domain

The simplified geometry (Figure 1b) was designed using CAD software (ANSYS Workbench Design Modeler®) following the actual shape of a Canada goose [19] in flight position. The wings were modeled using a two-joint arm model [19] that provides a simplified reproduction of the wing-flapping dynamics. Many studies consider that the overall shape of a bird's wing is that of a NACA profile [20-21] because the wings function like an airfoil, i.e. a curved surface that produces lift while minimizing turbulence in its wake. We, therefore, used a NACA 4412 profile whose aerodynamic performance was evaluated in the study by Malik et al. [22]. The distance between the geometry and the limits of the domain was defined to respect the recommendations published in the CFD best practice guidelines [23], which resulted in a blocking ratio lower than 3. The dimensions of the computational domain, as well as the boundary conditions, are shown in Figure 1(c).

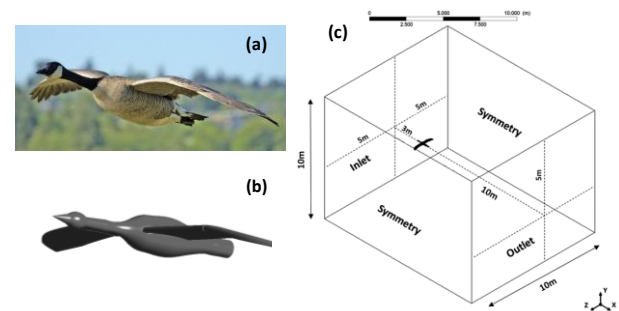


Fig. 1: (a) A Canada goose in flight (Photo Alan D.Wilson — Wikimédia); (b) Simplified geometry of the Canada goose. (c) Computational domain size and boundary conditions.

#### 2.1.1 Boundary Conditions

At the entrance of the computational domain, we imposed a speed of 50 km/h (13.9 m/s) which corresponds to the average speed of the Canada geese during a migratory flight [24]. At the exit of the computational domain, we imposed a pressure exit condition with the ambient static pressure. A symmetry condition was imposed on the upper and lateral surfaces of the computational domain.

Table 1. Numerical parameters and dimensional features of a Canada goose [24-25]. Numerical values were determined assuming that the bird is flying at an altitude of 1000 m [26].

Variable	Value
<b>Chord length (<math>c</math>)</b>	0.21 m
<b>Wing size</b>	0.82 m
<b>Flight speed (<math>U_\infty</math>)</b>	13.9 m/s
<b>Wingbeat frequency</b>	4 HZ
<b>Wingbeat amplitude</b>	0.6 m
<b>Wingspan</b>	1.8 m
<b>Flight altitude</b>	1000 m

An air density of 1.11 kg/m<sup>3</sup>, corresponding to an altitude of 1000m, was used as a reference value for the calculation [26]. The CFD parameters, as well as the dimensional parameters of the wing, are summarized in Table 1.

#### 2.1.2 Flapping Motion Modeling

We modeled the wing motion based on the wing-flapping dynamics of a bird in flight [19] (Fig. 2). Birdwing flapping is complex and involves several rotational movements, each of which influences the flight mechanics. For simplification, this study focuses only on the main rotational movement of the wings while neglecting the rotation of the leading edge of the wing which influences the thrust force.

The average wing flapping frequency of a Canada goose is about 4 Hz [24-25, 27-30]. To describe the real-time evolution of the wings' motion, a dynamic mesh has been adopted allowing to update of the wings' position at each time step ( $\Delta t=0.001s$ ). The updating of the volumetric mesh is automatically performed by the FLUENT solver and consists of a local remeshing that mainly uses an interpolation method to regenerate the mesh in the computational area, which is suitable for large and complex movements. Considering the amplitude of the wing's motion, we chose to use the spring-based smoothing and local re-meshing methods. The trajectory of the wings, which consists of an up and down rotational movement, has been implemented in the computational code through User Defined Functions (UDF).

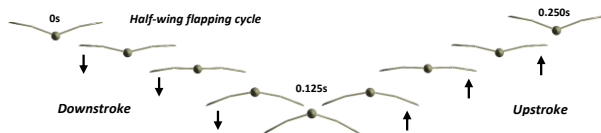


Fig. 2: Kinematics of a complete cycle of wing beats. Black arrows pointing upwards represent the upstroke phase while the black arrows pointing downwards represent the downstroke phase. The half-arrow represents the change in wing-flapping direction during the wingbeat cycle.

## 2.2 Meshing Methods

The three-dimensional grid of the computational domain was created with the ANSYS Workbench Meshing software (Figure 3). The unstructured mesh of the fluid domain is composed of approximately  $9 \times 10^6$  prismatic and hexahedral elements. The boundary layer grid requires a very fine mesh close to the wall to completely resolve the viscoelastic and laminar sub-layer. To correctly reproduce the boundary layer separation, an inflation layer composed of 15 layers of a progressive thickness (growth ratio: 1.2) was generated around the body wall (Figure 3c). To obtain a  $Y^+$  value lower than 1, necessary for a precise resolution of the boundary layer, the size of the cells adjacent to the wall around the bird's body has been adjusted to a value of  $10 \mu m$ . In addition, a mesh refinement zone was created around and in the wake of the bird. In this zone, the average size of the elements is less than or equal to  $0.05 m$ . Outside of this area, a Cartesian mesh is used, allowing to reduce the number of elements and consequently the calculation time.

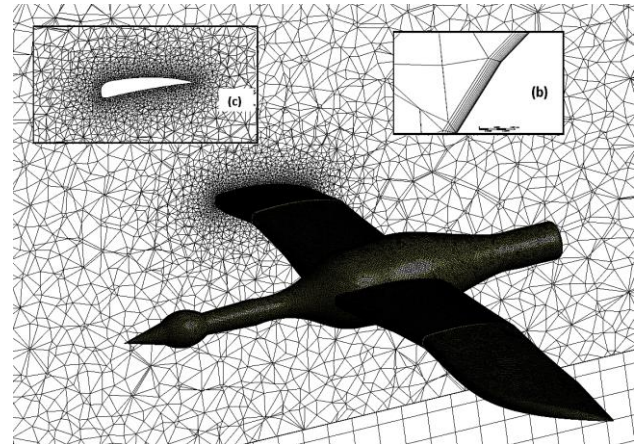


Fig. 3: Surface mesh on the bird's body and in a 2D vertical plane intersecting a wing of the bird (a); detail of the mesh around the wing in the shape of a NACA profile (b) and detailed view of the inflation mesh (c) around the wings.

## 2.3 Numerical Methods

The calculations were performed using the CFD code ANSYS Fluent<sup>®</sup> 2020 R2. The SST model  $k-\omega$  was used to solve the Reynolds Averaged Navier-Stokes (RANS) equations in 3D [31]. The simple algorithm was used for pressure-velocity coupling with second-order discretization schemes and gradients computed using the least-squares cell-based method. The SST turbulence model  $k-\omega$  is a two-equation model that is used for many aerodynamic applications. This turbulence model is fully adapted to unfavorable pressure gradients and separation flow and is therefore ideally suited for aerodynamic studies. [32-33]. The drag and lift coefficients were monitored throughout the iterative calculation. The calculations were performed on a Dell Workstation Precision 7920 workstation and were parallelized on 48 Xeon Gold 3.2 GHz processors. Note that the methodology used in this paper is fully described in a previous paper as well as the validation of the numerical results [34].

## 3 Results and Discussion

Four forces act on a flying device, whether it is a bird, bat, insect, or airplane: lift, thrust, drag, and gravity (Figure 4). Thrust must be equal to drag and lift must be equal to gravity in straight and level flight. In the study of flapping wings, several parameters can be used to quantify the flow characteristics. The most representative ones are presented below. Two parameters that provide important information in the study of flapping wings propulsion are the drag and lift coefficients, they are defined as follows:

$$C_D = \frac{D}{\frac{1}{2}\rho U^2 A} \quad (1)$$

$$C_L = \frac{L}{\frac{1}{2}\rho U^2 A} \quad (2)$$

$D$ ,  $L$  and  $T$  are the forces of drag, lift, and thrust (identical to the forces of drag but of opposite sign), respectively;  $\rho$  is the density of the fluid,  $U$  is the forward velocity, and  $A$  is the projected area ( $m^2$ ).

With the sole exception of the hummingbird, birds generate lift and thrust by flapping their wings, a complex, unstable, three-dimensional wing movement that changes with each new wing position. The flapping is performed in two phases: the downstroke, or power stroke, which produces much of the thrust, and the upstroke, or recovery stroke, which, depending on the bird's wing, produces a certain amount of lift. Of course, wings not only generate lift and thrust, but they also induce drag. Lift and drag are two components of the resulting aerodynamic force acting on the wing. The effective magnitude of the resultant aerodynamic force depends mainly on the magnitude of the flapping speed of the wing [35]. The lift can act in any direction relative to gravity since it is defined as the direction of flow rather than the direction of gravity. When a bird flies in a straight line, most of the lift is opposite to gravity [36]. However, when a bird climbs, descends, or tilts in a turn, the lift is inclined concerning the vertical.

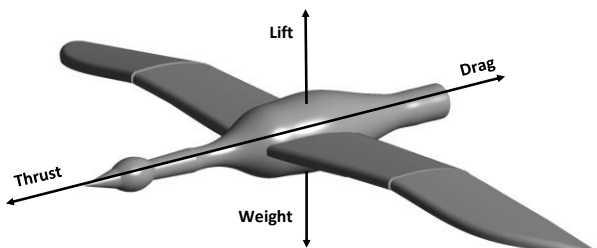


Fig. 4: Aerodynamic forces acting on a bird in flight.

Figure 5 depicts the variation of the lift and drag coefficients throughout a wing-flapping cycle. As shown in Figure 5, the lift coefficient is maximum at mid-downstroke and minimum at mid-upstroke. The drag coefficient is minimal at mid-downstroke and maximal between mid-upstroke and the start of the downstroke. On the other hand, the drag coefficient becomes negative during the downstroke, indicating that reverse drag forces are generated and then lift forces are increased during the downstroke. We can also see that the lift coefficient becomes negative in

the upstroke, indicating that inverse lift forces are generated, and then drag forces are increased during the upstroke. On the other hand, we can also see that the negative lift coefficient is larger than the negative drag coefficient.

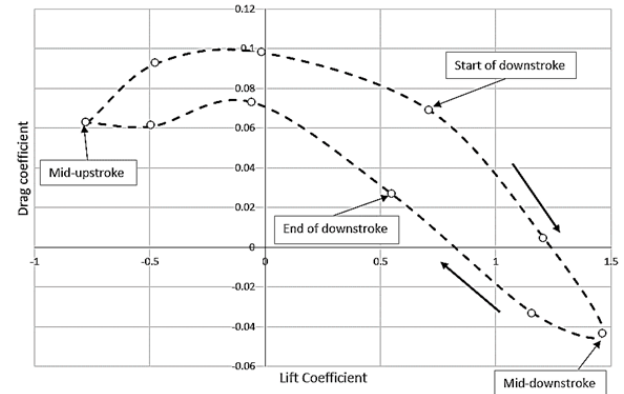


Fig. 5: Evolution of the lift and drag coefficients during one flapping cycle.

### 3.1 Pressure

Pressure is the normal force per unit area exerted by the air on itself and on the surfaces it hits. The lift force is transferred by the pressure, which acts perpendicular to the surface of the wing. Thus, the net force is expressed in the form of pressure differences. The direction of the net force implies that the average pressure on the upper surface of the wing is lower than the average pressure on the lower surface [37].

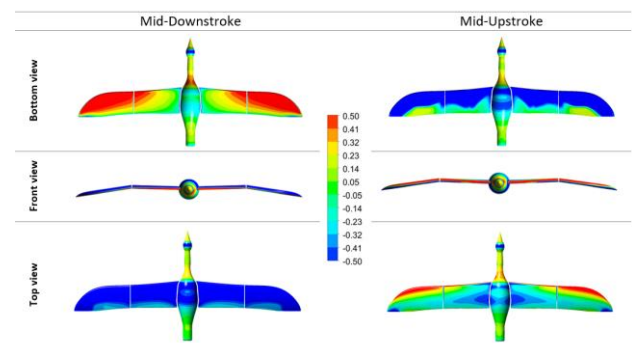


Fig. 6: Pressure coefficients on the bird's body and wings at  $t=0.125s$  (Mid-downstroke) and at  $t=0.25s$  (Mid-upstroke).

Figure 6 shows the distribution of pressure on the bird's body and wings at  $t=0.125s$  (Mid-downstroke) and  $t=0.25s$  (Mid-upstroke). Note that the pressure range has been deliberately limited to the interval  $[-0.5, 0.5]$  to highlight the slightest change in pressure. During the downstroke, the air collides with the underside of the wing, generating lift. During this



phase, the pressure is positive on the underside of the wing and negative on the upper phase. During the upstroke phase of the wing, the opposite happens, the pressures are globally positive on the top of the wing (extrados) while they are negative on the bottom (intrados). Moreover, we can see that the positive and negative pressures are maximum at  $t=0.125s$  (Mid-downstroke), which corresponds to the maximum lift (see Fig. 5). It is also remarkable that the highest pressures are at the wingtips, where the vortices develop. The lowest pressure occurs on the upper surface of the wing and the highest pressure under the wing.

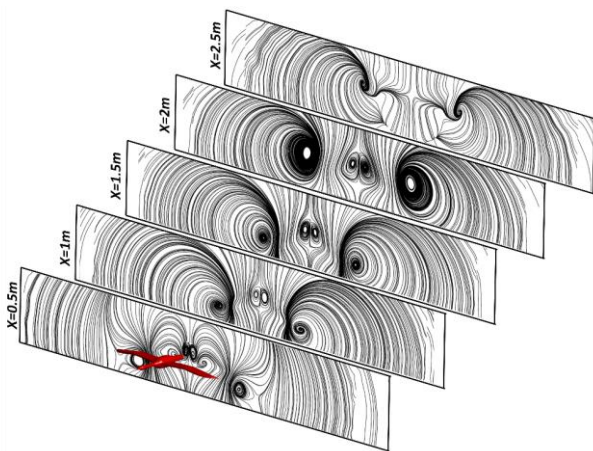


Fig. 7: Streamlines displayed in a vertical plane at 0.5m, 1m, 1.5m, and 2m respectively in the wake behind the bird and for the mid-upstroke position.

This pressure differential causes the airflow to turn back behind the wing, which in turn causes the airflow to rotate downstream of the wingtips. Once the reversal is completed, the wake consists of two counter-rotating cylindrical vortices.

These vortices are generated during the downstroke phase of high aspect ratio wings [38] and will be discharged with the downstream airflow. This couple of vortices pulls the air downwards, generating lift in the opposite direction. The wake develops while the wing is flapping up and down and especially during the downstroke, the induced vortices then play a considerable role.

Green [37] identified three mechanisms that describe the origin of wingtip vortices. The first and most common mechanism is the pressure imbalance at the tip, during the lift generation process. The pressure difference accelerates the flow from the pressure side (lower surface) to the suction side (upper surface), leading to the formation of a vortex at the wingtip (or simply at the tip). The strength of the vortex depends on the magnitude of the pressure

difference, which in turn depends on the angle of attack. For more information, figure 7 shows the streamlines of the flow in the bird's wake, drawn in 4 parallel vertical planes equidistant of 0.5m. The bird's wake is made up of two main structural parts: a pair of wingtip vortices and a pair of tail vortices. We can clearly distinguish the two counter-rotating vortices that developed at the wingtips. We can also see that the vortices eventually dissipate, their energy being transformed by viscosity. In addition, we used a volume rendering method that provides an overview of the three-dimensional structure of the vortex wake while giving quantitative information on vorticity. Figure 8 shows the volumetric representation of the wake behind the bird at two instants of the upstroke and downstroke phases. Note that the range of vorticity plotted along the x-axis (in the direction of the bird's movement) has been deliberately limited to the interval  $[-100; 100]$  to show the slightest change in vorticity intensity. The colors red and blue indicate that the vortices have an opposite direction of rotation, one vortex at the wingtip circulates clockwise while the other circulates counterclockwise. The two wingtip vortices do not merge because they flow in opposite directions. The wingtip vortices come up from the wingtips and tend to dive and roll over each other downstream of the wing. Again, the tip vortices eventually dissipate, their energy being transformed by viscosity. We can also see that when the bird flaps its wings, the trail of upwash left by the wingtips moves up and down in a wave-like motion related to the flapping of the wings.

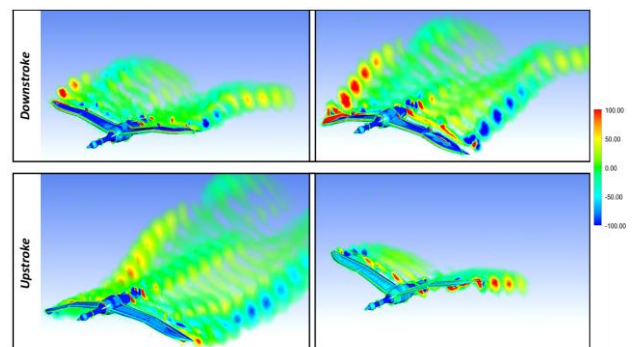


Fig. 8: Reconstruction of the approximate shape and movement of the vortex wake by the volume rendering method for two different moments during the Upstroke and Downstroke phases. Color refers to x-vorticity intensity.

### 3.2 Influence of Wake Flow on Migratory Bird Flight

When a bird is flying, a rotating air vortex separates from each wingtip. These vortices imply that the air

inside the vortex system, in the immediate wake of the bird, moves downwards (downwash) while the air on the sides, outside the vortex system, moves upwards (upwash).

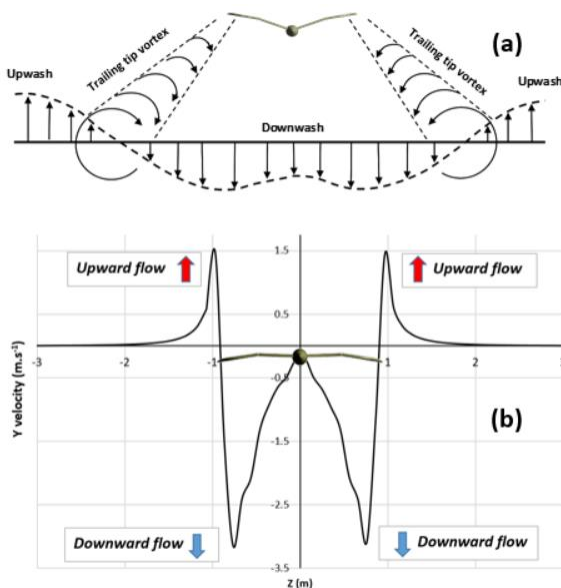


Fig. 9: schematic diagram of the vortex flow developing in the wake of a large bird flying at high speed (a). Radial velocity profile  $U_y$  plotted along an axis passing through the core of the vortex flow at  $x=1.5\text{m}$  and for Mid-downstroke (b).

Figure 9 (a) shows a schematic diagram of the airflow in the wake of a bird. Figure 9 (b) shows the vertical velocity plotted along a horizontal line passing through the core of the vortex flow at  $x=0.5\text{m}$  in the wake of the bird (for mid-downstroke).

From the graph, we can evidence two distinct zones: the upwash zone, in which the velocities are positive, and the downwash zone, in which the velocities are negative. Some studies suggest a close relationship between the position of birds in groups during formation flights and the flow topology in the wake of birds in flight [39-40]. Concretely, this means that in specific flight formations (such as V formations), the bird that flies in the wake of another bird could take advantage of upward currents and improve its lift, which would reduce its energy cost. This is the reason why many species of large birds fly in a V formation because the interest of collaborative flight is to reduce energy expenditure and improve the locomotor performance of the birds in the group [41-42]. The study by Portugal et al. [41] suggests that birds flying in V formation would have phasing strategies to cope with the dynamic wakes produced by wing flapping. Our results seem to confirm this observation. The oscillation of the vortex flow in the

wake of the bird suggests that phasing of the wing flapping of the following bird with the preceding bird is necessary to reduce energy expenditure. In future numerical studies, it will be possible to study the aerodynamic interaction between several birds flying in formation but also the influence of wing flapping phasing on the forces acting on the birds in flight.

## 4 Conclusion

In this study, we modeled the unsteady flow around and in the wake of a large flying bird by including realistic wing flapping kinematics. A CFD method was used to highlight the three-dimensional vortex structures developing in the wake of a Canada goose flying at an altitude of 1000m and a speed of 13.9m/s. Post-processing of the 3D results revealed a complex vortex flow whose main structure is composed of two contra-rotating vortices developing at the wingtip. From flow velocity fields, we highlighted two distinct zones: the upwash zone, in which the flow is ascending and the velocities are positive, and the downwash zone, in which the flow is descending and the velocities are negative. It seems that migratory birds use the area of upward currents to improve lift and save energy costs during a migration. Furthermore, it has been shown that when the bird flaps its wings, the trail of upwash left by the wingtips also moves up and down in a wave-like motion. The unsteady wake dynamics suggest that when migratory birds fly in formation, phasing of the wing-flapping between the follower and the lead bird is necessary to benefit from a reduction in energy expenditure. To our best knowledge, this study is the first to provide a detailed and realistic representation of the unsteady three-dimensional wake of a large migratory bird during a flapping flight. Further studies, which will include several birds flying together, will be necessary to understand the full aerodynamic implications of migratory birds flying in formation.

## References:

- [1]. Couzin I. D., Krause J., Franks N.R. & Levin S.A., Effective leadership and decision making in animal groups on the move. *Nature*, Vol. 433, 2004, pp. 513–516.
- [2]. Nagy M., Akos Z., Biro D. & Vicsek T., Hierarchical group dynamics in pigeon flocks. *Nature*, Vol. 464, 2010, pp. 890–894.
- [3]. May R.M., Flight formations in geese and other birds. *Nature*, Vol. 282, 1979, pp. 778–780.

- [4]. Lissaman P.B. & Schollenberger C.A., Formation flight of birds. *Science*, Vol. 168, 1970, pp. 1003–1005.
- [5]. Liao J.C., Beal D.N., Lauder G.V. & Triantafyllou M.S., Fish exploiting vortices decrease muscle activity. *Science*, Vol. 302, 2003, pp. 1566–1569.
- [6]. Bill R.G. & Hernnkind W.F., Drag reduction by formation movement in spiny lobsters. *Science*, Vol. 193, 1976, pp. 1146–1148.
- [7]. Weimerskirch H., Martin J., Clerquin Y., Alexandre P. & Jiraskova S., Energy saving in flight formation. *Nature*, Vol. 413, 2001, pp. 697–698.
- [8]. Fish F.E., Kinematics of ducklings swimming in formation: consequence of position. *J. Exp. Zool.*, Vol. 273, 1995, pp. 1–11.
- [9]. Badgerow J. P. & Hainsworth F.R., Energy savings through formation flight? A reexamination of the vee formation, *J. Theor. Biol.*, Vol. 93, 1981, pp. 41–52.
- [10]. Cutts C.J. & Speakman J. R., Energy savings in formation flight of pink-footed geese, *J. Exp. Biol.*, Vol. 189, 1994, pp. 251–261.
- [11]. Hummel D., Aerodynamic aspects of formation flight in birds, *J. Theor. Biol.*, Vol. 104, 1983, pp. 321–347.
- [12]. Maeng J.S. et al., Park J.H., Min Jang S., Han S.Y., A modelling approach to energy savings of flying Canada geese using computational fluid dynamics, *J. Theor. Biol.*, Vol. 320, 2013, pp. 76–85.
- [13]. Magnan A., Perrilliat-Botonet C., Girerd H., Essais d'enregistrements cinématographiques simultanées dans trois directions perpendiculaires d'exu à de l'écoulement de l'air autour d'un oiseau en vol, *C. r. hebdomadaire des séances Acad. Sci. Paris*, Vol. 206, 1938, pp. 462–464.
- [14]. Spedding G.R., Hedenström A. & Rosén M., Quantitative studies of the wakes of freelyflying birds in a low-turbulence wind tunnel, *Experiments in Fluids*, Vol. 34, 2003, pp. 291–303.
- [15]. Spedding G.R., Rosén M. & Hedenström A., A family of vortex wakes generated by a thrush night ingale in free flight in a wind tunnel over its entire natural range of flight speeds, *Journal of Experimental Biology*, Vol. 206, 2003, pp. 2313–2344.
- [16]. Nafi A.S., Ben-Gida H., Guglielmo C.G., Gurka R., Aerodynamic forces acting on birds during flight: A comparative study of a shorebird, songbird and a strigiform, *Experimental Thermal and Fluid Science*, Vol. 113, 2020, p. 110018.
- [17]. D. Michael., Animal locomotion: a new spin on bat flight. *Curr. Biol.*, Vol. 18, 2008, pp. 468–470.
- [18]. Song J, Tobalske BW, Powers DR, Hedrick TL, Luo H., Three-dimensional simulation for fast forward flight of a calliope hummingbird, *R. Soc. Open sci.*, Vol. 3, 2016, p. 160230.
- [19]. Liu T., Kuykendoll K., Rhew R.D., Jones S., Avian Wings, AIAA, 2004, pp. 2004–2186.
- [20]. Shyy W., Berg M., Ljungqvist D., Flapping and flexible wings for biological and micro air vehicles, *Prog. Aerosp. Sci.*, Vol. 35, 1999, pp. 455–505
- [21]. Usherwood J.R., Hedrick T.L., Biewener A.A., The aerodynamics of avian take-off from direct pressure measurements in Canada geese (*Branta canadensis*), *J. Exp. Biol.*, Vol. 206, 2003, p. 4051.
- [22]. Malik K., Aldheeb M., Asrar W., Erwin S., Effects of Bio-Inspired Surface Roughness on a Swept Back Tapered NACA 4412 Wing, *J Aerosp Technol. Manag.*, Vol. 11, 2019, p. e1719.
- [23]. Blocken B., Computational Fluid Dynamics for urban physics: Importance, scales, possibilities, limitations and ten tips and tricks towards accurate and reliable simulations, *Building and Environment*, Vol. 91, 2015, pp. 219–245,
- [24]. Tucker V.A., Schmidt-Koenig K., Flight speeds of birds in relation to energetics and wind directions, *The Auk*, Vol. 88, 1971, pp. 97–107.
- [25]. Funk G. D., Milsom W.K., Steeves J.D., Coordination of wingbeat and respiration in the Canada goose. I. Passive wing flapping. *Journal of applied physiology*, Vol. 73, n°3, 1992, pp. 1014–1024.
- [26]. Fergus C., Canada goose. Wildlife Notes-20, LDR0103, Pennsylvania Game Commission, 2010.
- [27]. Gould L.L., Heppner F., The vee formation of Canada geese, *The Auk*, Vol. 91, n°3, 1974, pp. 494–506.
- [28]. Hainsworth F., Induced drag savings from ground effect and formation flight in brown pelicans, *J. Exp. Biol.*, Vol. 135, 1988, pp. 431–444.
- [29]. Hedrick T.L., Tobalske B.W., Biewener A.A., Estimates of circulation and gait change based on a three-dimensional kinematic analysis of flight in cockatiels (*Nymphicus hollandicus*)

- and ringed turtle-doves (*Streptopelia risoria*), *J. Exp. Biol.*, Vol. 205, 2002, p. 1389.
- [30]. Tennekes H., *The Simple Science of Flight: From Insects to Jumbo Jets*, MIT Press, Cambridge, MA, 1996.
- [31]. Menter F.R., Zonal two-equation k-to turbulence model for aerodynamic flows, AIAA Paper 1993–2906. AIAA 1993-2906, 23rd Fluid Dynamics, Plasma dynamics, and Lasers Conference, 1993.
- [32]. Polidori G., Legrand F., Bogard F., Madaci F., Beaumont F., Numerical investigation of the impact of Kenenisa Bekele's cooperative drafting strategy on its running power during the 2019 Berlin marathon, *Journal of Biomechanics*, Vol. 107, 2020, p. 109854.
- [33]. Fintelman D.M., Hemida H., Sterling M., Li F.-X., CFD simulations of the flow around a cyclist subjected to crosswinds, *Journal of Wind Engineering and Industrial Aerodynamics*, Vol. 144, 2015, pp. 31-41.
- [34]. Beaumont F., Murer S., Bogard F., Polidori G., Aerodynamics of a flapping wing as a function of altitude: New insights into the flight strategy of migratory birds, *Physics of Fluids*, Vol. 33, 2021, p. 127118.
- [35]. Dvořák R., Aerodynamics of bird flight, *EPJ Web of Conferences*, Vol. 114, 2016, p. 01001.
- [36]. Hoerner S.F. & Borst H.V., *Fluid-dynamic Lift: Practical Information on Aerodynamic and Hydrodynamic Lift*, L.A. Hoerner, 1985.
- [37]. Green S.I., *Wing Tip Vortices, Fluid Vortices*, Kluwer Academic Publishers, Netherlands, 1995.
- [38]. Hedenström A., Spedding G.R., Beyond robins: aerodynamic analyses of animal flight, *J. Royal Soc.: Interface*, Vol. 5, 2008, pp. 595-601.
- [39]. Weimerskirch H., Martin J., Clerquin Y., Alexandre P., Jiraskova S., Energy saving in flight formation, *Nature*, Vol. 413, 2001, pp. 697–698.
- [40]. Hummel D., Aerodynamic aspects of formation flight in birds, *J. Theor. Biol.*, Vol. 104, 1983, pp. 321–347.
- [41]. Portugal S. J., Hubel T. Y., Fritz J., Heese S., Trobe D., Voelkl B., Hailes S., Wilson A. M., Usherwood J. R., Upwash exploitation and downwash avoidance by flap phasing in ibis formation flight. *Nature*, Vol. 505, 2014, pp. 399–402.
- [42]. Lissaman P.B.S., Shollenberger C.A., Formation Flight of Birds, *Science*, Vol. 168, n°3934, 1970, pp. 1003–1005.

### **Contribution of Individual Authors to the Creation of a Scientific Article (Ghostwriting Policy)**

Fabien Beaumont performed the simulations and optimization and wrote the original draft.

Guillaume Polidori performed the investigation, analysis, and validation.

Sébastien Murer and Fabien Bogard provided supervision and review.

### **Sources of Funding for Research Presented in a Scientific Article or Scientific Article Itself**

There are no sources of funding.

### **Creative Commons Attribution License 4.0 (Attribution 4.0 International, CC BY 4.0)**

This article is published under the terms of the Creative Commons Attribution License 4.0

[https://creativecommons.org/licenses/by/4.0/deed.en\\_US](https://creativecommons.org/licenses/by/4.0/deed.en_US)